Subaperture stitching interferometry for testing a large hyperboloid

WANG Xiao-kun[1], ZHENG Li-gong[1], ZHANG Bin-zhi[1,2], YAN Feng[1,2], ZHANG Zhong-yu[1], ZHANG Xue-jun[1]

(1.Key Laboratory of Optical System Advanced Manufacturing Technology,Changchun Institute of Optics, Fine Mechanics and Physics, Chinese Academy of Sciences, Changchun 130033, China;
2.Graduate School of the Chinese Academy of Sciences, Beijing 100039, China)

Abstract: In order to test large aspheric surfaces without the aid of null optics, a novel method called subaperture stitching interferometry (SSI) is presented. The synthetical optimization stitching model are established based on homogeneous coordinate′s transform and simultaneous least-squares fitting. A prototype of testing large aspheres is developed by the stitching method. The experiment of testing a hyperboloid with SSI is carried out. The PV and RMS of the surface are 0.319λ and 0.044λ (is 632.8 nm) respectively when five subapertures are stitched together. For comparison and validation, the asphere is also measured by null testing. It is shown that the two testing results consist with each other, PV and RMS error are 0.032λ and 0.004λ respectively. Thus, it can be concluded that the algorithm and model of the SSI technology are feasible for the testing of large aspheric surfaces, which provides the probability of testing the mirror with large aperture and asphericity in non-null configuration.

Key words: Optical metrology; SSI; Aspheric surface; Least-squares fitting

CLC number:TN247 **Document code:**A **Article ID:**1007-2276(2009)01-0114-06

子孔径拼接干涉测量一大口径双曲面

王孝坤[1],郑立功[1],张斌智[1,2],闫 锋[1,2],张忠玉[1],张学军[1]

(1.中国科学院长春光学精密机械与物理研究所 中国科学院光学系统先进制造技术重点实验室,吉林 长春 130033;2.中国科学院研究生院,北京 100039)

摘 要:为了无需辅助元件就能够实现对大口径非球面的检测,将子孔径拼接技术与干涉技术相结合,提出了一种利用子孔径拼接干涉检测非球面的新方法。分析了该技术的基本原理,并基于齐次坐标变换、最小二乘拟合建立了一种综合优化的拼接模型,在此基础上初步设计和搭建了子孔径拼接干涉检测装备。利用该方法对一口径为 350 mm 的双曲面进行了 5 个子孔径的拼接检测,得到拼接后的全口径面形误差的 PV 值为 0.319λ,RMS 值为 0.044λ(=632.8 nm)。为了对比和验证,对该非球面进行了零位补偿检测,两种方法测量所得的全口径面形分布是一致的,其 PV 值和 RMS 值的偏差分别为 0.032λ 和 0.004λ。实验结果表明:该数学模型和拼接算法是准确可行的,从而提供了一种非零补偿测试大口径非球面的手段。

关键词:光学检测; 子孔径拼接干涉; 非球面; 最小二乘拟合

收稿日期:2008-04-05; **修订日期**:2008-06-10

基金项目:中国科学院长春光学精密机械与物理研究所三期创新基金资助项目

作者简介:王孝坤(1980-),男,江苏丹阳人,助理研究员,博士,主要从事光学超精加工和检测技术研究。Email:jimwxk@sohu.com

0 Instruction

Aspheric surfaces have the ability of correcting aberrations and improving image quality besides reducing the size and weight of the optical system [1-4]. As the application of aspheres in optical systems becomes more and more prevalent, the accurate and efficient testing of these surfaces is needed imminently. Interferometry is the most important testing technology because of its high resolution, high sensitivity and repeatability, which has become the standard tool for testing optical surfaces and wavefronts. For the testing of aspheric surfaces with large aperture and steep departure, auxiliary optics such as null corrector and CGH(computer generated hologram) must be applied to prevent too dense interference fringes and improper non-unique errors. However, these auxiliary elements need to be designed and manufactured specially, which increases the total fabricating time and cost. Furthermore, fabricate errors and misalignment errors of these auxiliary optics will be introduced to the workpiece. Subaperture stitching technology can expand both the longitudinal and the lateral dynamic ranges of interferometer as well as broaden the measuring scope significantly [5-7]. Therefore, SSI provides an effective method for testing aspheric surfaces, which can be used for measuring large-aperture, small f-number aspheric surfaces at high resolution, low cost and high efficiency without null optics.

1 Theory

The sketch and the flow chart of SSI are given in Fig.1 and Fig.2, respectively. Firstly, the surface under test, particularly its nominal aperture and radius of curvature should be defined. Then proper standard lens should be selected and the size and number of the subaperture should be determined according to the surface under test[8]. Secondly, the phase distribution of the central subaperture is recorded when the two

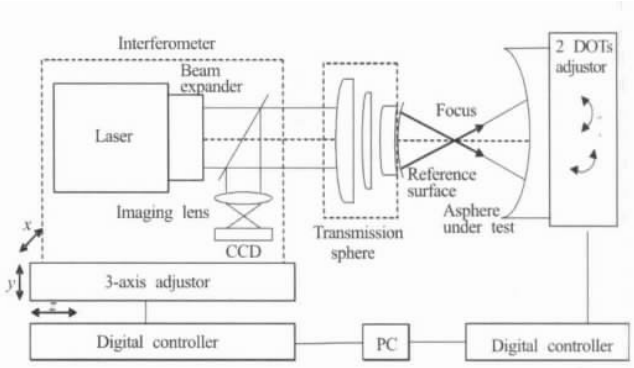

Fig.1 Sketch of the setup for testing asphere by SSI

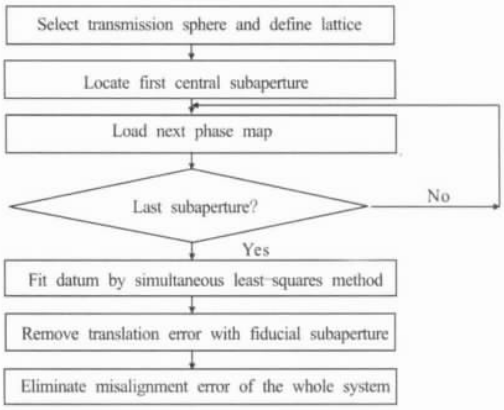

Fig.2 Flow chart of SSI

centers of curvature of the testing spherical wavefront and the best-fit-sphere of the central subaperture are adjusted to coincided with each other by manipulating the relative location of interferometer and the surface under test accurately. Thirdly, the phase distribution of the marginal subapertures is obtained one by one when the testing wavefront of interferometer matches the correct subaperture on the surface by adjusting their relative positions carefully. Great attention should be paid to two key points: one is that the slope of the testing wavefront should be adjusted to match the slope of corresponding subaperture, and the other is that adjacent subapertures should have enough overlapping areas. Fourthly, the central subaperture is selected to be the fiducial area and the data of all the subapertures is unified into the fiducial area by homogeneous coordinate's transform. Finally the relative translation error of corresponding subaperture introduced by the least-square method is eliminated by minimizing the

discrepancy on the overlapping areas. After all the translation errors are subtracted, a least-squares fitting is performed to evaluate the misalignment errors of the whole system. Thus, the final wavefront error map is obtained.

2 Stitching algorithm

The relative translation errors must be eliminated when two corresponding subapertures are stitched. All the subapertures can be stitched together by adding a new subaperture iteratively to the main part ,which has been stitched according to the principle of two subapertures stitching, and it often suffers from the stackup error [9]. A new method that stitching all the subapertures together simultaneously is developed to avoid this kind of error in this paper. For the sake of localization and measurement simplicity, the central subaperture is selected generally to be the fiducial subaperture.

Supposing that there are M subapertures totally, each measurement needs to hold the following function for the correction of tilt, power and piston:

$$\begin{aligned} w_0 &= w_1 + a_1 x_1 + b_1 y_1 + c_1 (x_1^2 + y_1^2) + d_1 = \\ & w_2 + a_2 x_2 + b_2 y_2 + c_2 (x_2^2 + y_2^2) + d_2 = \\ & \vdots \\ & w_{M-1} + a_{M-1} x_{M-1} + b_{M-1} y_{M-1} + c_{M-1} (x_{M-1}^2 + y_{M-1}^2) + d_{M-1} \end{aligned} \tag{1}$$

Where w_0 is the phase distribution of the fiducial subaperture ;$w_1, w_2, \cdots, w_{M-1}$ are the phase distributions of other subapertures.

Least squares fitting algorithm as shown in formula (2) is adopted to minimize the differences in the overlapping areas between adjacent subapertures:

$$\begin{aligned} S = \sum_{j_1 \neq 0}^{N_1} \sum_{i_1 \subset W_0, W_{j1}}^{n} \{ & W_0(x_{1i_1}, y_{1i_1}) - [W_{j_1}(x_{j_1 i_1}, y_{j_1 i_1}) - a_{j_1} x_{j_1 i_1} - b_{j_1} y_{j_1 i_1} - \\ & c_{j_1}(x_{j_1 i_1}^2 + y_{j_1 i_1}^2) - d_{j_1}]\}^2 + \sum_{j_2 I\ j_3 \neq 0}^{N_2} \sum_{i_2 \subset W_{j2}, W_3}^{n} \{[W_{j_2}(x_{j_2 i_2}, y_{j_2 i_2}) - a_{j_2} x_{j_2 i_2} - \\ & b_{j_2} y_{j_2 i_2} - c_{j_2}(x_{j_2 i_2}^2 + y_{j_2 i_2}^2) - d_{j_2}] - [W_{j_3}(x_{j_3 i_2}, y_{j_3 i_2}) - a_{j_3} x_{j_3 i_2} - b_{j_3} y_{j_3 i_2} - \\ & c_{j_3}(x_{j_3 i_2}^2 + y_{j_3 i_2}^2) - d_{j_3}]\}^2 = \min \end{aligned} \tag{2}$$

Where W_0 is the phase distribution of the fiducial subaperture;$(x_{1i_1}, y_{1i_1}), (x_{j_1 i_1}, y_{j_1 i_1}), (x_{j_2 i_2}, y_{j_2 i_2}), (x_{j_3 i_2}, y_{j_3 i_2})$ denote the unified reference coordinate of each subaperture;a_j, b_j, c_j, d_j are ordinally the coefficients of the four relative translation error terms that are x-tilt, y-tilt, power and piston compared with the fiducial subaperture;N_1 is the number of subapertures that overlaps the fiducial subaperture; N_2 is the number of subapertures that overlaps the other subaperture excluding the fiducial subaperture, thus the total number of the overlapping areas is N_1+N_2; n is the number of sampling points of each common region.

The best splicing parameters can be obtained by formula(3), which is the differentiation form of formula (2) with respect to these unknowns.

$$\begin{cases} \dfrac{\partial S}{\partial a_i} = 0 \\ \dfrac{\partial S}{\partial b_i} = 0 \\ \dfrac{\partial S}{\partial c_i} = 0 \\ \dfrac{\partial S}{\partial d_i} = 0 \end{cases} \tag{3}$$

The coordinate frame of the subaperture is shown in Fig.3, where (x_0, y_0, w_0) is the coordinate frame of the

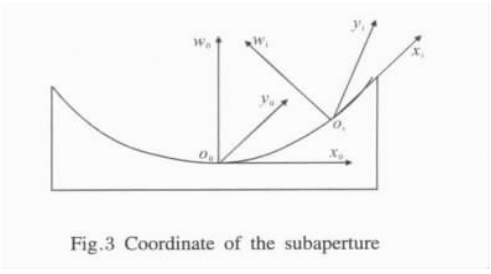

Fig.3 Coordinate of the subaperture

fiducial subaperture while (x_i, y_i, w_i) is the coordinate of other subapertures. According to homogeneous coordinate′s transform, the relationship between them can be expressed as formula (4):

$$(x_0, y_0, w_0, 1) = (x_i, y_i, w_i, 1) \cdot V \tag{4}$$

Where V is the transposition matrix that can be described as follows:

$$V = T \cdot R \cdot S \tag{5}$$

Where T is the matrix of translation. Supposing the relative translations to the fiducial subaperture in the X, Y and W directions are P_x, P_y, and P_w, respectively, it can be expressed as formula (6):

$$T=T_x\cdot T_y\cdot T_w=\begin{bmatrix}0&0&0&0\\0&1&0&0\\0&0&1&0\\P_x&0&0&1\end{bmatrix}\begin{bmatrix}1&0&0&0\\0&1&0&0\\0&0&1&0\\0&P_y&0&1\end{bmatrix}\begin{bmatrix}1&0&0&0\\0&1&0&0\\0&0&1&0\\0&0&P_x&1\end{bmatrix}=\begin{bmatrix}1&0&0&0\\0&1&0&0\\0&0&1&0\\P_x&P_y&P_w&1\end{bmatrix} \tag{6}$$

Where R is the matrix of rotation. Supposing the relative rotations to the fiducial subaperture in the X,Y and W directions are α, β, and γ, respectively, it can be expressed as formula (7):

$$R=R_x\cdot R_y\cdot R_w=\begin{bmatrix}1&0&0&0\\0&\cos\alpha&\sin\alpha&0\\0&-\sin\alpha&\cos\alpha&0\\0&0&0&1\end{bmatrix}\begin{bmatrix}\cos\beta&0&-\sin\beta&0\\0&1&0&0\\\sin\beta&0&\cos\beta&0\\0&0&0&1\end{bmatrix}\begin{bmatrix}\cos\gamma&\sin\gamma&0&0\\-\sin\gamma&\cos\gamma&0&0\\0&0&1&0\\0&0&0&1\end{bmatrix}=$$
$$\begin{bmatrix}\cos\beta\cos\gamma&\cos\beta\sin\gamma&-\sin\beta&0\\\sin\alpha\sin\beta\cos\gamma-\cos\alpha\sin\gamma&\sin\alpha\sin\beta\sin\gamma+\cos\alpha\cos\gamma&\sin\alpha\cos\beta&0\\\cos\alpha\sin\beta\cos\gamma+\sin\alpha\sin\gamma&\cos\alpha\sin\beta\sin\gamma-\sin\alpha\cos\gamma&\cos\alpha\cos\beta&0\\0&0&0&1\end{bmatrix} \tag{7}$$

Because the asphere under test is rotational-symmetric, γ is equal to zero. S is the matrix of scale. Because the zoom of CCD is the same as each subaperture, S is set to 1.

Hence the phase data of all the subapertures can be unified to the same benchmark and stitched together by formula(3)~(7).

After all the relative translation errors are eliminated, a least-squares fitting is implemented to evaluate the misalignment errors of the system as formula (8) shows:

$$\sum_{i=1}^{N}\{\Phi_i(x_i,y_i)-[Ax_i+By_i+C(x_i^2+y_i^2)+D]\}^2=\min \tag{8}$$

Where Φ_i is the phase distribution over the full aperture; N is the number of total sampling points; A,B,C,D are the misalignment coefficients that can be obtained by the following formula:

$$\begin{bmatrix}A\\B\\C\\D\end{bmatrix}=\begin{bmatrix}\sum xx&\sum xy&\sum x(x^2+y^2)&\sum x\\\sum yx&\sum yy&\sum y(x^2+y^2)&\sum y\\\sum(x^2+y^2)x&\sum(x^2+y^2)y&\sum(x^2+y^2)^2&\sum(x^2+y^2)\\\sum x&\sum y&\sum(x^2+y^2)&N\end{bmatrix}^{-1}\begin{bmatrix}\sum x\Phi\\\sum y\Phi\\\sum(x^2+y^2)\Phi\\\sum\Phi\end{bmatrix} \tag{9}$$

The reafter the accurate figure error of the asphere can be derived finally after these misalignment errors are removed.The elaborate stitching algorithm and numerical simulations are described in another paper[10].

3 Experiment

A hyperboloid is tested to verify the proposed

mathematical model and the stitching algorithm. The hyperboloid under test is well polished, with a clear aperture of 350 mm and a radius of curvature of 4 180 mm approximately. The conic constant is −2.816 915. The experimental setup is shown in Fig.4. There are 5 DOFs totally that can be adjusted. The Zygo interferometer is mounted on the *X*/*Y*/*Z* translation stage, while the asphere is mounted on a two axes stage ,which offers freedom of tip and tilt to be adjusted accurately. The whole setup is mounted on a vibration isolator.

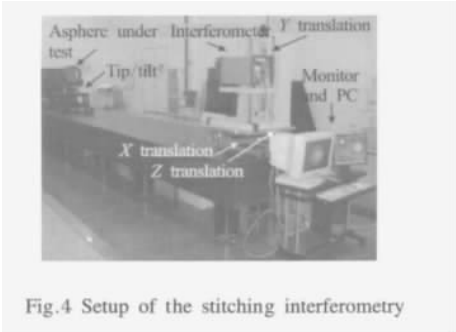

Fig.4 Setup of the stitching interferometry

A lattice design tha t covers the whole surface under test with five subapertures is illustrated in Fig.5,

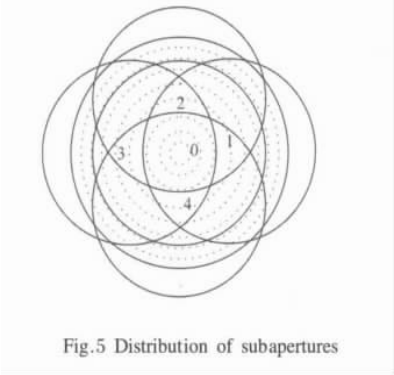

Fig.5 Distribution of subapertures

where a single subaperture is about eighty percent of the full aperture. The results of the five individual measurements (the fiducial subaperture, the central subaperture and four outer subapertures) are given in Fig.6. Then all the subapertures are unified into the same coordinate frame by homogeneous coordinate transform and translation errors are eliminated from each subaperture by the least-squares method. After all the translation errors are removed, a final least-square fitting is performed to evaluate the misalignment errors of the whole system. The misalignment coefficients are

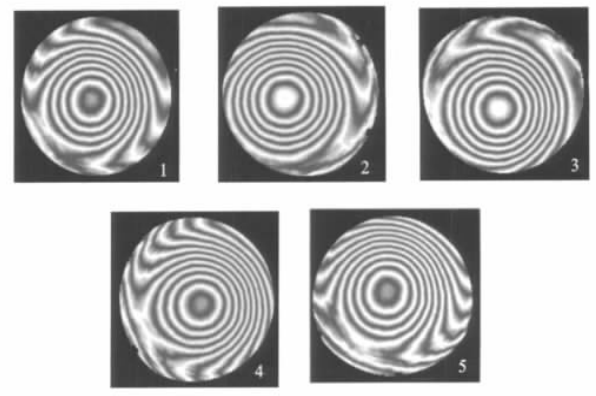

(a) Interferograms of five subapertures

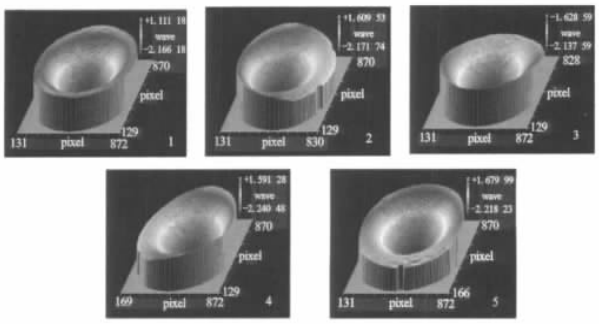

(b) Corresponding phase distributions of five subapertures

Fig.6 Testing results of five subapertures

showed in Tab.1 and the exact figure error of the asphere can be obtained by eliminating these errors.

Tab.1 Misalignment errors of the system

	Piston	*X*/tilt	*Y* /tilt	Power
Misalignment coefficients	8.427 0e−004	−9.342 1e−003	−1.806 6e−003	1.843 4e−003

The surface map of the reconstructed full aperture is given in Fig.7, where the PV error is 0.319λ and the RMS error is 0.044λ.

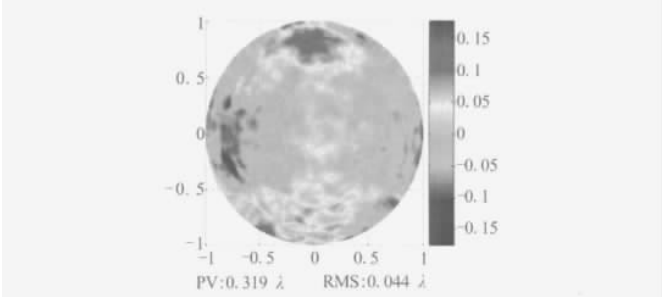

Fig.7 Normalized surface map of the whole aperture after stitching

In order to validate the accuracy of SSI technology,

the hyperboloid is also tested by null compensation for comparison. The interferogram and phase map of the null test are shown in Fig.8, where the PV and RMS

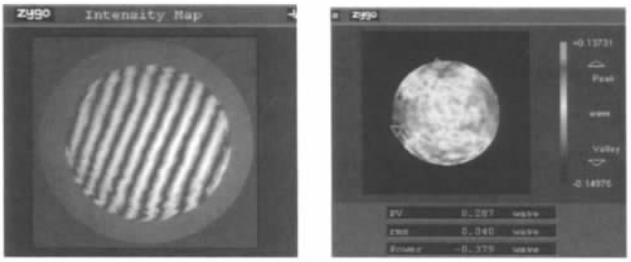

Fig.8 Interferogram and surface map of null compensation

are 0.287λ and 0.040λ, respectively. It can be calculated that the difference of PV and RMS error of these two methods is 0.032λ and 0.004λ respectively and it can be seen that the surface maps obtained by these two methods are coincide well with each other. Furthermore, the PV and RMS of residual error of phase distribution of these two methods are calculated. The map of the residual error is given in Fig.9, where $PV_{(\delta w)}$=0.132λ, $RMS_{(\delta w)}$=0.012λ.

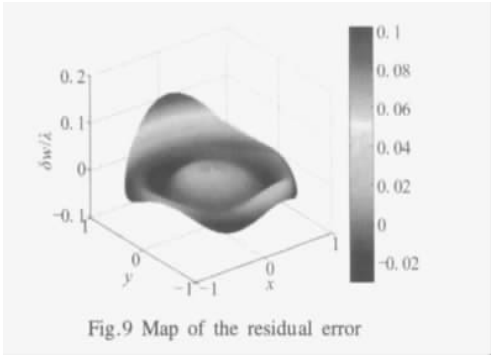

Fig.9 Map of the residual error

Although only five subapertures were required to cover the full aperture in this experiment, the same stitching procedure can be applied to test those larger and deeper aspherical surfaces with more subapertures.

4 Conclusion

SSI can test large aspheric surfaces with high resolution and high efficiency without null optics. The synthetical optimization stitching model is presented in this paper. The stitching algorithm based on a simultaneous least-squares proposed can minimize the mismatch error among all overlapping regions, which prevents the error transmitting and accumulating. The data processing and mathematical operation are efficient. The results of the SSI testing experiment validate that this mathematical model and stitching algorithm are feasible. The projection distortion is very small because of the small asphericity of the surface under test, thus the non-common path errors can be eliminated by subtracting the theoretical wavefront error from the phase data. But when the surfaces with large asphericity are tested, the projection distortion and non-common error should be considered carefully. The calibration process will become more complicated, which needs future research.

References:

[1] MALACARA D. **Optical Shop Testing** [M].2nd ed. New York: J Wiley&Sons,1992.

[2] HTROYUKI K. Influence of system aberrations on interferometric aspheric syaface testing [C]// **Proceedings of SPIE**, 1986, **680**:47-52.

[3] ZHANG Xue-jun,LI Zhi-lai,ZHANG Zhong-yu. Space telescope aspherical mirror structure design based on SiC material [J]. **Infrared and Laser Engineering**, 2007,**36** (1): 192-198. (in Chinese)

[4] LIU Hua,LU Zhen-wu,LI Feng-you,et al.CGH testing for large concave surface [J].**Infrared and Laser Engineering**, 2007,**36**(2):192-198.(in Chinese)

[5] NEGRO J E. Subaperture optical system testing[J].**Appl Opt**, 1984,**23**(12):1921-1930.

[6] JON F,PAUL D, PAUL E M,et al.An automated subaperture stitching interferometer workstation for spherical and aspherical surfaces [C]//**Proceedings of SPIE, Advanced Characterization Techniques for Optics, Semiconductors, and Nanotechnologies**,2003,**5188**:296-307.

[7] ARIC S,WILLIAM K, MARC T.Magnetorheological finishing and sub-aperture stitching interferometry of large and lightweight optics [C]//**Proceedings of SPIE,Optical Fabrication, Metrology, and Material Advancements for Telescopes**, 2004,**5494**:81-90.

[8] MARC T,PAUL D,GREG F.Sub-aperture approaches for asphere polishing and metrology [C]//**Proceedings of SPIE, Optical Design and Testing II**,2005,**5638**:284-299.

[9] MASASHI O, KATSUYUKI O, JUMPEI T.Measurement of large plane surface shapes by connecting small-aperture interferograms[J].**Opt Eng**,1994,**33**(20):608-613.

[10] WANG Xiao-kun,WANG Li-hui,ZHANG Xue-jun.Testing asphere by subaperture stitching interferometric method [J]. **Optics and Precision Engineering**,2007,**15** (2):192-198. (in Chinese)